Molecular Crystals and Liquid Crystals
Publication details, including instructions for authors and subscription information:
http://www.tandfonline.com/loi/gmcl16

New Liquid Crystal Materials; Physical Properties and Performance in Displays for Automobile, High Information Density and Guest-host Applications

M. Schadt [a], M. Petrzilka [a], P. R. Gerber [a], A. Villiger [a] & G. Trickes [a]
[a] Central Research Units, F, HOFFMANN-LA ROCHE & CO., Ltd., 4002, Basel, Switzerland
Version of record first published: 21 Mar 2007.

To cite this article: M. Schadt , M. Petrzilka , P. R. Gerber , A. Villiger & G. Trickes (1983): New Liquid Crystal Materials; Physical Properties and Performance in Displays for Automobile, High Information Density and Guest-host Applications, Molecular Crystals and Liquid Crystals, 94:1-2, 139-153

To link to this article: http://dx.doi.org/10.1080/00268948308084253

Mol. Cryst. Liq. Cryst., 1983, Vol. 94, pp. 139–153
0026-8941/83/9402–0139/$18.50/0

Printed in the United States of America

New Liquid Crystal Materials; Physical Properties and Performance in Displays for Automobile, High Information Density and Guest-host Applications

M. SCHADT, M. PETRZILKA, P. R. GERBER, A. VILLIGER, and G. TRICKES

Central Research Units, F. HOFFMANN-LA ROCHE & CO., Ltd. 4002 Basel Switzerland

(Received October 22, 1982)

Four novel liquid crystal classes are presented, namely bi-, tri-, and tetracyclic ethanes, pyridazines, and tetracyclic chloro-diesters. Each class exhibits distinct physical characteristics, such as low viscosities $\eta \sim 12$ cP, low elastic ratios $k_{33}/k_{11} \sim 1$, large mesomorphic ranges ~40°C. . . .250°C, large negative dielectric anisotropies $\Delta\varepsilon \lesssim -9$ and/or low dielectric relaxation frequencies $f_c \sim 1$ kHz. It is shown that the dielectric Debye relaxation time τ characterizing the hindered rotation of polar nematic molecules around their short axes is much more affected by molecular structural factors than by their rotational viscosity γ_1. The material and electro-optical properties of mixtures for twisted nematic and guest-host LCDs comprising the new compounds are presented. The mixtures cover a wide range of applications such as high contrast, fast and multiplexable automotive TN-LCDs; positive and negative contrast guest-host LCDs; high-information density matrix, and dual-frequency addressable LCDs.

I. INTRODUCTION

The remarkable development of liquid crystal display (LCD) technology since the early 1970's and the subsequent extended use of devices comprising liquids other than electrolytes by the electronics industry, is closely connected with (i) the discovery of electro-optical field effects, (ii) liquid crystal (LC) material research, and (iii) the development of new, reliable, and increasingly sophisticated LCD-production-technologies. Field-effect LCDs based on the twisted nematic effect[1] (TN-LCDs), as well as on several guest-host effects[2–4] (GH-LCDs), are today being used in an increasing variety of applications. From the beginning of this development, especially

in today's most advanced applications, LC-mixtures are required containing LC-components whose specific physical properties[5] have to be combined such that optimal electro-optical properties result. Thus, physical and chemical LC-material research is a prerequisite for the discovery of new LC-classes contributing to improved performance of existing LCD's or to open up new applications. Such a role was played, for example, by LC-classes such as the cyano Schiff'bases,[6] the cyano biphenyls,[7] and the cyano phenylcyclohexanes,[8] to mention just a few of historically important classes.

We believe that the interesting properties of LCDs can be further improved during this decade by developing new LC-materials and by further developing the LCD technology. Therefore, and because of the rapid development of microelectronics, LCDs are expected to find, for example, new applications in automobiles (dashboards), computers (very high information density, large area matrix LCDs), and related fields. However, in order for LCDs to meet the stringent technological demands of these new applications, novel LC-materials are required. For example, the present multiplexing capability of LCDs which are limited by LC-material properties[5] has to be improved considerably if high contrast and high-information density LCDs with as few as possible electrode connections are to be realized.

In the following, four new liquid crystal classes will be presented and compared with some existing compounds. Each of the classes is shown to exhibit distinct elastic, viscous, mesomorphic, as well as static and dynamic dielectric properties. The new compounds are shown to contribute to interesting electro-optical properties in conventionally, as well as, dual-frequency addressed TN-LCDs, and in negative, as well as, positive contrast GH-LCDs. Mixtures made of the new materials are presented covering automotive as well as high-information density applications. Some of the new materials open up the possibility of improving the multiplexability of TN-LCDs to an extent which by far exceeds that of the best conventionally addressable LC-materials. Moreover, guest-host materials are presented that open up the possibility to multiplex GH-LCDs.

2. NEW CLASSES OF LIQUID CRYSTALS

The nine components depicted in the upper part of Table I are novel liquid crystals belonging to a number of homologous series recently synthesized in our laboratories. They can be divided into four classes, each exhibiting

TABLE I

The abbreviations C, P and A stand for cyclohexyl ring, phenyl ring, and ethane linkage respectively, whereas the numbers refer to the numbers of carbon atoms in a straight alkyl chain. T_m = melting temperature; T_{S-N} = smectic-nematic transition temperature, where the indices *A*, *B* and *C* refer to the respective smectic phases; T_{S-I} = smectic-isotropic transition; T_{N-I} = nematic-isotropic transition.

Nomenclature	T_m [°C]	T_{S-N} (S-I) [°C]	T_{N-I} [°C]	Structure	Ref
5CAP3	4	$(18)_B$	-	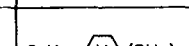	novel liquid crystals
α =5CAPO2	18	-	46	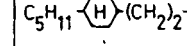	
α_1=5CPAC4	28	$(138)_A$	-	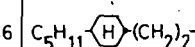	
α_2=5CPAPAC4	33	$(188)_A$	-	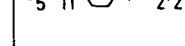	
α_3=5CPPAC4	41	$(239)_A$	258	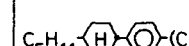	
5PZH3	66	-	12	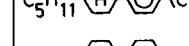	
A7	128	-	291	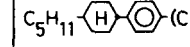	
B_17	115	129_C	258	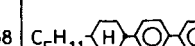	
B_27	141	-	255	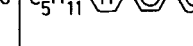	
$5EH_2O3$	43	-	72		[14]
5CAC5	46	$(109)_B$	-	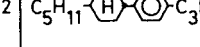	[11]
4CPO2	47	-	31		[9]
3CPPC5	54	251_A	312	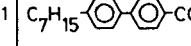	[10]
TP_3H_32	118	-	222	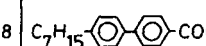	[16]

distinct physical characteristics, which, if adequately combined, lead to mixtures with interesting electro-optical properties covering a wide range of applications, some of which are novel. In the following, data on a number of material parameters are presented, such as static and dynamic dielectric properties, viscous, elastic, and optical constants. The measurements were made either by using single components or, in case of non-overlapping mesomorphic ranges, by using simple mixtures.

The first class of new structures depicted in Table I comprises the *phenylcycloethyl ethanes* denominated 5CAP3 and 5CAPO2. We show below that ethanes exhibit very low viscosities. Considering the rather flexible ethane linkage of the two rings, it seems rather astonishing that the nonpolar bicyclic compound 5CAPO2 exhibits a quite large and purely nematic mesophase (Table I). This is all the more surprising if one considers that rigid phenylcyclohexanes[9] with comparable side chains are monotropic (see 4CPO2 at the bottom of Table I). The dialkyl substituted bicyclic ethanes such as 5CAP3 depicted in Table I were found to exhibit pure smectic B mesophases, i.e. except for the width their mesomorphic behavior resembles that of the bicyclohexylethanes[11] (see 5CAC5 at the bottom of Table I).

The second class of new compounds shown in Table I contains the *tri-* and *tetracyclic ethanes* denominated α_1, α_2, and α_3; i. e. molecules with elongated cores. Table I shows that α_1, α_2, and α_3 have, despite their considerable core flexibility, surprisingly large mesophases and high isotropic transition temperatures. Because of the additional core flexibility, T_{NI} of α_2 and α_3 are not as large as those of the tetracyclic biphenylcyclohexyl[10] 3CPPC5 depicted at the bottom of Table I. Moreover, increasing the number of ethane linkages (see α_2 and α_3 in Table I) and/or shifting a single ethane group (from its position in α_3) into the center of the core causes the transition temperature to decrease markedly. Because of the low viscosity, good solubility and high isotropic transition temperatures tri- and tetracyclic ethanes were found to be useful additives for increasing the nematic-isotropic transition temperature of mixtures without adversely affecting their viscosity. Both of the above classes of ethanes are extraordinarily stable against UV-irradiation and/or extended exposure to high temperatures.

The monotropic *pyridazine* denominated 5PZH3 in Table I belongs to the third class of new compounds. Compared with the other classes, compounds of this type were found to exhibit, due to the lateral permanent dipole moments in the pyridazine ring, large negative dielectric anisotropies (Table II). Pyridazines will be shown below to induce useful dielectric, as well as, viscous properties in strongly negative dielectric anisotropic hosts designed for positive contrast guest-host LCDs.

TABLE II

The dielectric, optical and elastic constants $\varepsilon_\parallel$, $\Delta\varepsilon$, n_{0°, Δn, k_{11} and k_{33}/k_{11} were measured at constant reduced temperature (T_{NI} − 10°C), whereas the bulk viscosity η was measured at 22°C = constant. Mixture N_1 contains the components N_1 = (4EH$_2$O2, 4EH$_2$O5, 5EH$_2$O1, 5EH$_2$O3, 5CPACO2) in molar proportions (21%, 26, 19, 21, 13). The rotational viscosity of N_1 at 22°C is γ_1 = 1.06P.

Composition [weight %]		T_m [°C]	T_{N-I} [°C]	$\varepsilon_\parallel$	$\Delta\varepsilon$	n_0	Δn	k_{11} [x1O^{-12} N]	k_{33}/k_{11}	η (22°C) [cP]
5CAPO2	[100]	18.0	46.0	2.67	−0.26	1.483	0.074	10.12	1.06	12.9
5EH$_2$O3	[100]	43.3	71.7	3.09	−0.82	1.469	0.061	6.24	0.96	29.0
(5EH$_2$O3, 5CAPO2)	[91,9]	< 35	67.4	3.01	−0.78	1.473	0.063	6.56	0.90	27.5
N_1	[100]	< −5	64.9	3.13	−0.77	1.479	0.061	6.31	0.96	24.4
(N_1, α_1)	[91,9]	< −5	70.4	3.01	−0.65	1.479	0.061	6.04	0.96	27.1
(N_1, α_2)	[91,9]	< −5	76.4	3.03	−0.65	1.480	0.062	6.51	0.99	27.3
(N_1, α_3)	[91,9]	<−10	81.5	3.08	−0.58	1.480	0.062	5.64	0.98	29.4
(N_1, TP$_3$H$_3$2)	[91,9]	< −5	72.2	5.94	1.55	1.481	0.067	5.60	1.01	35.2
5PZH3	[100]	66	12	8.2	−9.3	—	—	—	—	—
(N_1, 5PZH3)	[91,9]	< −5	60.5	3.51	−1.37	1.479	0.061	6.05	0.98	24.3

The fourth class of new structures comprises the rather unusual *tetracyclic chloro-diesters* A7, B$_1$7, and B$_2$7 (Table I). These are strongly positive dielectric anisotropic compounds and they contribute, as we have recently shown,[12] to rather unique dielectric phenomena, if properly combined with other liquid crystals such as pyridazines. Representatives of this class are used in novel, dual-frequency addressable mixtures (see paragraph 3 and Refs. 12 and 13).

Table II shows measurements of the static dielectric constants $\varepsilon_\parallel$ and $\Delta\varepsilon = (\varepsilon_\parallel - \varepsilon_\perp)$, the optical anisotropy $\Delta n = (n_e - n_o)$, the splay elastic constant k_{11}, the elastic ratio k_{33}/k_{11}, where k_{33} = bend elastic constant, and the bulk viscosity η. The measuring methods used were described earlier.[5] To allow comparisons, the dielectric, optical, and elastic properties were determined at constant (reduced) temperature (T_{NI} − 10°C), whereas η was measured at T = 22°C = constant. The data of the monotropic pyridazin component 5PZH3 were obtained by extrapolating from measurements made with binary mixtures (5EH$_2$O3, 5PZH3) of varying molar proportions. To investigate the influence of some of the new compounds on the viscosity and the nematic-isotropic transition temperature of other liquid crystals, "binary" mixtures of the type (N_1, X) were studied, where N_1 is a low viscosity mixture whose composition is given in the text of Table II.

Comparing the data of the first three lines in Table II shows that the viscosity of the unpolar bicyclic phenylcycloethane 5CAPO2 is more than a factor of 2 lower than η of the low viscosity and also unpolar cyclohexyl ester[14] 5EH$_2$O3 (Table I). A similar factor holds with respect to the

viscosities[15] of the polar cyano phenylcyclohexanes[8] (PCHs) and the cyano biphenyls.[7] As to the optical anisotropy, Table II shows that Δn of phenylcyclohexylethanes is similar to that of other bicyclic compounds containing one hydrogenated ring.[5] With respect to the elastic ratios k_{33}/k_{11}, it is interesting to note the small values of bicyclic as well as tri- and tetracyclic ethanes (Table II) which, compared with a large number of other liquid crystal classes,[5] are among the smallest. Since k_{33}/k_{11} was shown[5] to crucially affect the steepness of the transmission characteristics of TN-LCDs, the low k_{33}/k_{11}, values of ethanes are indicative of their attractive multiplexing properties (see paragraph 3.1).

Comparing the increase of T_{NI} and of η occurring upon doping mixture N_1 with the tri- and tetracyclic ethanes α_1, α_2, and α_3 respectively, shows that η does not increase by more than 20% despite strong increases of T_{NI} (Table II). To further illustrate this aspect, Table II also contains data of mixture (N_1, TP_3H_32) comprising the polar terpyrimidine TP_3H_32[16]) (Table I). TP_3H_32 causes T_{NI} to increase only moderately compared with the associated strong increase of η (Table II).

The results obtained from the pyridazine mixture (N_1, 5PZH3) at the bottom of Table II show that 5PZH3 hardly affects η of mixture N_1. This finding indicates that the strongly negative dielectric anisotropic pyridazines exhibit, unlike molecules with external lateral polar substituents, low viscosities; however, 5PZH3 is strongly monotropic, thus depressing T_{NI} of N_1 upon doping (Table II).

The strongly hindered rotation of nematic molecules around their short axes leads to the dispersion of the parallel dielectric constant $\varepsilon_\parallel(f)$ with increasing frequency.[17] At the cross-over frequency f_c the positive dielectric anisotropy $\Delta\varepsilon(f)$ can become zero. Increasing f further causes $\Delta\varepsilon(f)$ to change sign. Thus, in the dispersion region considered here, the following low-frequency dielectric properties can be defined:[12] $\Delta\varepsilon_L = \Delta\varepsilon(f \ll f_c)$, $\varepsilon_\perp$ = constant, $\varepsilon_\infty = \varepsilon_\parallel(f \gg f_c)$, $\Delta\varepsilon_H = (\varepsilon_\infty - \varepsilon_\perp)$, and the Debye relaxation time $\tau = 1/\omega_o$ determined by the angular frequency where $\varepsilon_\parallel(\omega_o) = (\varepsilon_\parallel + \varepsilon_\infty)/2$. We could recently show for the first time that mixtures comprising, for example, tetracyclic chloro diesters can be made that exhibit extremely low cross-over frequencies as well as large and adjustable dielectric anisotropies $\Delta\varepsilon_L$ and $\Delta\varepsilon_H$ respectively.[12] The question arises to what extent the surprisingly low f_c-values are related with molecular structural elements, as well as with the bulk and rotational viscosities η and γ_1 of mixtures containing such components. Figure 1 shows dielectric relaxation measurements carried out at constant reduced temperature (T_{NI} − 55°C) using mixture N_1 containing either A7, B_17, B_27, or TP_3H_32 (Table I). The dielectric data of these four mixtures obtained from Figure 1 are depicted in Table III. Because T_{NI} of the mixtures are comparable

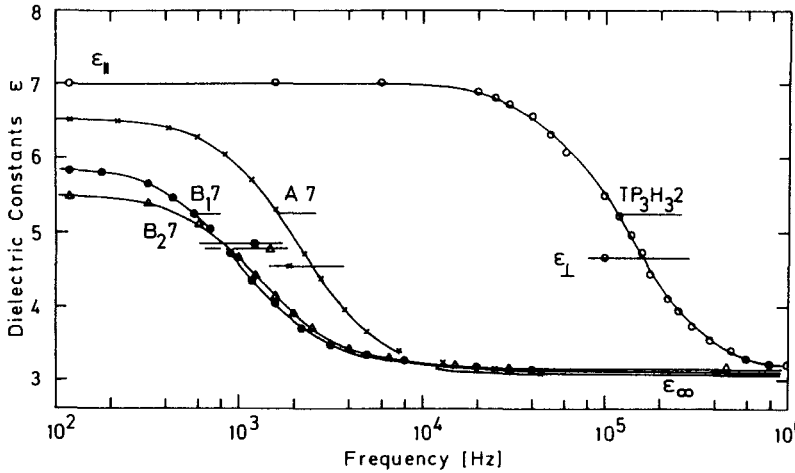

FIGURE 1 Frequency dependence $\varepsilon_{\parallel}(f)$ determined at (T_{NI} − 55°C) of mixtures (N_1, A_7), (N_1, B_1), (N_1, B_2) and (N_1, TP_3H_32) respectively. Since $\varepsilon_{\perp}(f)$ = constant over the frequency range studied, only the crossings of $\varepsilon_{\perp}$ with the respective $\varepsilon_{\parallel}(f)$-graphs are shown.

(Table III), the reduced measuring temperatures (T_{NI} − 55°C) chosen are all close to room temperature. The results in Figure 1 and Table III show that the tetracyclic diesters A7, $B_1$7, and $B_2$7 exhibit surprisingly low-lying dispersion regions compared with the terpyrimidine TP_3H_32. This finding is unlikely to be due only to the additional fourth ring in the diesters. It can certainly neither be attributed to the differences among the viscosities of the mixtures which are almost negligible compared with the two orders of

TABLE III

Physical properties of dual-frequency addressable materials; cf. text of TABLE II for the composition of N_1. All measurements were made at the reduced temperature (T_{NI} − 55°C) except those of the viscosities η and γ_1 that were made at T = 22°C = constant. τ = Debye relaxation time following from $\tau = 1/2\pi f_0$, where f_0 = frequency at $(\varepsilon_{\parallel} + \varepsilon_{\infty})/2$ (Figure 1). Mixture M is used as the host material in the black guest-host mixture denominated M_B.

Composition [weight %]		T_m [°C]	T_{NI} [°C]	$\varepsilon_{\parallel}$ (static data)	$\varepsilon_{\perp}$ (static data)	$\Delta\varepsilon_L$ (static data)	ε_{∞}	$\Delta\varepsilon_H$	f_c [kHz]	τ [x1O^{-5} sec]	η (22°C) [cP]	γ_1 (22°C) [P]
(N_1, A7)	[91,9]	~10	79.2	6.51	4.54	1.97	3.09	−1.45	2.50	7.58	36.8	1.77
(N_1, $B_1$7)	[91,9]	~10	78.1	5.86	4.84	1.02	3.11	−1.73	0.82	14.5	44.0	2.06
(N_1, $B_2$7)	[91,9]	~10	78.0	5.48	4.78	0.70	3.18	−1.60	0.90	11.79	43.0	1.91
(N_1, TP_3H_32)	[91,9]	< 5	72.2	7.00	4.67	2.33	3.22	−1.45	164	0.124	35.2	2.04
M	[100]	−10	74.5	10.25	8.30	1.95	3.90	−4.40	1.20	8.38	60.2	3.15
M_B = (M, black dye)	[96,4]	−10	77.8	9.95	8.12	1.83	3.88	−4.24	0.91	10.7	78.6	4.24

magnitude difference found between the relaxation times τ of the diester and the terpyrimidine mixtures respectively (Table III). Thus, our results show that dielectric relaxation models which almost exclusively relate τ with γ_1, such as suggested in reference 18, are not correct. It is interesting to note in Figure 1 that the f_c-values of the compounds $B_1 7$ and $B_2 7$ are comparable and almost three times smaller than f_c of A7. Thus, the methyl dicyano-vinyl end group of the *B* compounds (Table I) seems to affect f_c markedly, whereas hydrogenation of the terminal ring of $B_2 7$ affects f_c surprisingly little.

3. PERFORMANCE IN AUTOMOTIVE, HIGH-INFORMATION DENSITY AND GUEST-HOST LCDS

3.1. Automotive and conventionally addressable high-information density LC-materials

At first glance, the LC-material requirements for automotive LCD dashboards seem to be quite different from those of high information density matrix LCDs. Automotive dashboards have to be operated over very large temperature ranges; their optical contrast, especially in transmission, must be high and their response times fast, even at very low temperatures. On the other hand, LC-materials for conventionally addressed high-information density TN-LCDs have to exhibit excellent multiplexing properties. Thus, steep transmission characteristics with a small, or at least a linear temperature dependence over an often limited temperature range, are required. With respect to multiplexability and LC-material parameters, we have recently shown for a large number of LC-classes[5] that (i) nonpolar molecules tend to exhibit low elastic ratios k_{33}/k_{11} and that (ii) low values of k_{33}/k_{11} is an essential prerequisite for obtaining outstanding multiplexing properties at a given temperature. Therefore, and because nonpolar molecules are less viscous than their polar counterparts, mixtures with large mesomorphic ranges containing suitable nonpolar components are likely to perform better over the respective temperature ranges in both, automotive, as well as high information density LCDs. However, such relatively nonpolar mixtures will inevitably exhibit slightly increased threshold voltages.

By combining the ethanes presented above with positive dielectric and optically strong anisotropic LC-classes, mixtures with very low viscosities, large mesomorphic ranges, low elastic ratios k_{33}/k_{11} and rather high optical anisotropies were developed. Since the optical path difference $\delta = \Delta n \cdot d$ determining the contrast of a TN-LCD decreases with increasing temperature, large Δn-values lead, especially at high temperatures where Δn decreases, to improved results. Moreover, increased optical anisotropies

are compatible with small display gaps d, thus allowing to further reduce the response times of the LCD. Figure 2 shows the static (upper part) and the dynamic (lower part) transmission characteristics of a TN-LCD comprising the fast response and wide temperature range ethane-mixture 2706 from F. Hoffmann-La Roche. In agreement with the low k_{33}/k_{11}-values of 2706, Figure 2 shows that very steep characteristics are indeed obtained. From Figure 2 follows the maximum number N_{max} of multiplexable lines at a given temperature and vertical light incidence N_{max} (22°C) = 73; where

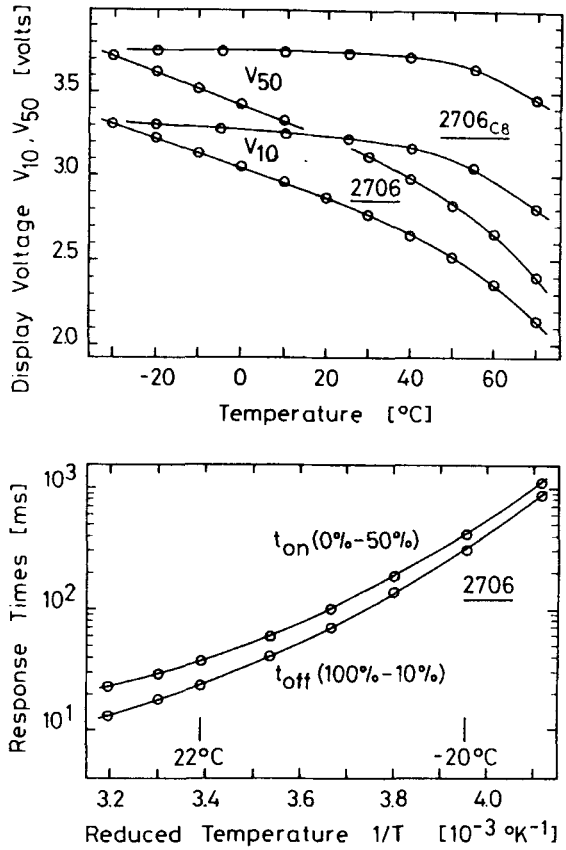

FIGURE 2 Static (upper part) and dynamic (lower part) transmission characteristics of low bias tilt TN-LCDs (cell gap d = 8 μm) comprising mixture 2706 and its temperature compensated counterpart 2706_{C8} respectively. Measurements made at vertical light incidence. Mixture 2706 exhibits the following data (at 22°C): η = 21.5 cP, k_{11} = 17.6 × 10^{-12} N, k_{22} = 7.71 × 10^{-12} N, k_{33}/k_{11} = 1.07, n_o = 1.497, Δn = 0.135, $\varepsilon_{\parallel}$ = 8.72, $\Delta\varepsilon$ = 5.40, T_m < −40°C and T_{NI} = 86°C.

$$N_{max} = \frac{[(p + 1)^2 + 1]^2}{[(p + 1)^2 - 1]^2}, \qquad p = \frac{(V_{50} - V_{10})}{V_{10}} \tag{1}$$

Because of the temperature dependence of the transmission characteristics, N_{max} decreases with increasing width of the operating temperature range if no external temperature dependent drive voltage regulation is used. Thus, if 2706 has to be multiplexed over the extreme temperature range from $-30°C$ to $+75°C$, i.e. over 105°C, one obtains N_{max} $(-30, +75°C) = 3.4$ from the static temperature dependence in Figure 2. This result shows that multiplexing of car dashboard LCDs is very difficult to achieve if no temperature compensation of the LCD characteristics is provided. To extend the good multiplexing properties of 2706 for TN-LCDs with 8 μm cell gaps over the above extreme temperature range, a well-defined temperature dependent left-handed pitch was induced[19] in 2706 by doping the mixture with suitable optically active additives. The upper part of Figure 2 shows the resulting considerably reduced temperature dependence of the compensated mixture denominated 2706_{C8}. Due to the compensation a remarkable increase of N_{max} (2706) = 3.4 to N_{max} $(2706_{C8}) = 9.7$ was achieved over the temperature range $-30°C$..... $+75°C$ (Figure 2).

From the dynamic data depicted in the lower part of Figure 2 follows, in accordance with the low viscosity of 2706 (see text of Figure 2), a short total response time $(t_{on} + t_{off}) \lesssim 700$ ms at $-20°C$. A detailed description of the electro-optical measuring conditions used can be found in Ref. 5.

3.2. Very high-information density, dual-frequency addressable LC-materials for twisted nematic LCDs

We have recently derived analytical approximations which describe the influence of LC-material properties on the static electro-optical performance of dual-frequency addressed LCDs. Moreover, LC-materials were developed which render dual-frequency addressing of LCDs applicable for the first time. As a result, remarkable improvements of the number of multiplexable lines of TN-LCDs by up to a factor of 30, compared with conventionally addressed TN-LCDs, were achieved.[12] The exceptionally low cross-over frequencies f_c and the large, as well as adjustable dielectric anisotropies $\Delta\varepsilon_L$ and $\Delta\varepsilon_H$ of the new mixtures are essentially due to the tetracyclic chloro diesters and pyridazines presented in paragraph 2 (Table I). Table III shows the dielectric and viscous data of such a dual-frequency addressable mixture denominated M.

Figure 3 shows static electro-optical characteristics of a TN-LCD comprising the dual-frequency mixture M (dashed graphs) as well as

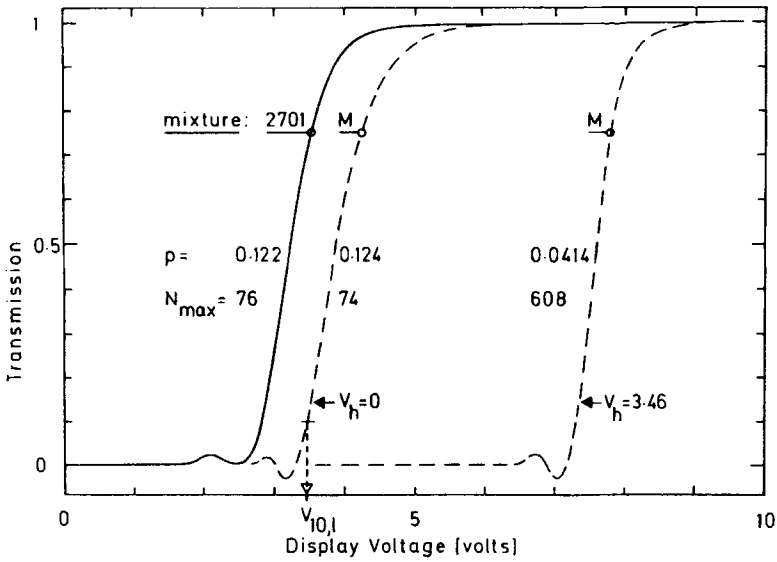

FIGURE 3 Static TN-LCD transmission characteristics at T = 22°C of the fast response, wide-range mixture 2701 and the dual-frequency addressable mixture M. The two graphs on the left were recorded with a driving frequency f_L = 80 Hz. The dashed graph on the right was recorded while superimposing a high-frequency voltage V_H (10 kHz)—where $V_H/V_{10,L}$ = 1 = constant—was superimposed on the TN-LCD comprising mixture M. The data on M are depicted in Table III, while those of 2701 (at 22°C) are: η = 24.8 cP, k_{11} = 18.5 × 10^{-12} N, k_{22} = 8.93 × 10^{-12} N, k_{33}/k_{11} = 1.17, n = 1.500, Δn = 0.142, $\varepsilon_\parallel$ 1 = 9.55, $\Delta\varepsilon$ = 6.19, T_m < −40°C and T_{NI} = 91°C.

characteristics of the low k_{33}/k_{11}-ratio, wide temperature range ethane-mixture 2701 (solid graph). Due to the low elastic ratios of M and 2701, both displays exhibit steep characteristics with N_{max} (2701) = 76 and N_{max} (M) = 74 respectively (Figure 3). The dashed graph on the left in Figure 3 was recorded while no high-frequency voltage V_H (10 kHz $\gg f_c$) was superimposed on the swept, low-frequency driving voltage V_L(80 Hz $\ll f_c$). Figure 3 shows that the superposition of the constant high-frequency voltage $V_H = V_{10,L}$ = 3.46 volts on V_L leads (i) to a shift of the characteristics of the TN-LCD comprising mixture M and (ii) to a steeper slope. As a consequence, the maximum number of multiplexable lines increases to N_{max} = 608! (dashed graph on the right in Figure 3). We have shown[12] that still larger N_{max} values can be obtained by either increasing the dielectric ratio $|\Delta\varepsilon_H/\Delta\varepsilon_L|$ of mixture M or by increasing V_H. This follows from the approximation[12]

$$p_H \cong \left[\frac{(p_L + 1)^2 + \frac{|\Delta\varepsilon_H|}{\Delta\varepsilon_L}\left(\frac{V_H}{V_{10,L}}\right)^2}{1 + \frac{|\Delta\varepsilon_H|}{\Delta\varepsilon_L}\left(\frac{V_H}{V_{10,L}}\right)^2} \right]^{1/2} - 1, \qquad (2)$$

where $p_L = p(V_H = 0)$ and $p_H = p(V_H \neq 0)$ is the parameter characterizing the slope of the dual-frequency addressed TN-LCD. Therefore, if one considers time-multiplexing ratios of 1:16 or 1:32 as state of the art with conventional high-multiplexing LC-materials (i.e. with elastic ratios $k_{33}/k_{11} \simeq 1.1$) the above results indicate that the information density of future TN-LCDs can reach those of plasma displays.

3.3. Negative and positive contrast guest-host-LCDs, dual-frequency addressable hosts

Because of the flat transmission characteristics of GH-LCDs comprising conventional nematic hosts and homogeneous, as well as homeotropic boundaries, the above LCDs could, so far, virtually not be multiplexed.[20] However, we have shown recently that dual-frequency addressable nematic, as well as cholesteric hosts, can be realized and that GH-LCDs exhibiting either positive or negative optical contrast can be made using such materials.[13] Negative optical contrast results if displays with homogeneous (parallel) wall alignment, driven by a low-frequency voltage $V_L(f_L \ll f_c)$ are used; whereas positive contrast is obtained in displays with homeotropic boundaries driven by a high-frequency voltage $V_H(f_H \gg f_c)$. Since in the case of negative contrast $\Delta\varepsilon_L > 0$ holds, the nematic director $\hat{n}$ of the host aligns parallel to an applied electric field $\hat{E}$ $(f_L \ll f_c)$; whereas, due to $\Delta\varepsilon_H < 0$ for $\hat{E}$ $(f_H \gg f_c)$, perpendicular alignment results with the same host in the positive contrast, dual-frequency addressable GH-LCD.

Figure 4 shows recordings of the transmission of a homogeneously aligned GH-LCD containing the dual frequency addressable black GH-mixture M_B (negative contrast graphs α and β). The data of M_B are summarized in Table 3. The black dyes used are similar to those reported earlier.[20] Also depicted in Figure 4 are recordings of the transmission of a homeotropically aligned GH-LCD containing the same mixture M_B (positive contrast graphs γ and δ). Moreover, to compare the positive contrast performance of M_B with a conventional negative dielectric anisotropic host, Figure 4 also shows the transmission of a homeotropically aligned, low viscosity and strongly negative dielectric anisotropic pyridazine GH-mixture N comprising the same amount of black dyes as M_B. The data of mixture N are summarized in the text of Figure 4. The dashed graph B in

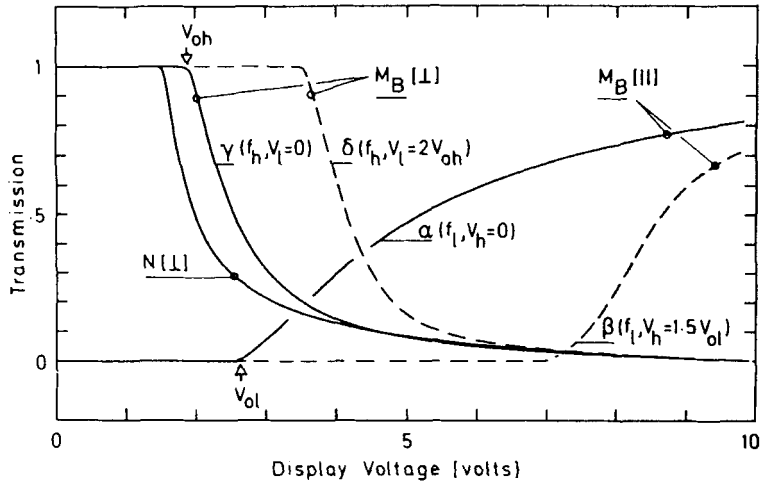

FIGURE 4 Transmission characteristics of two *homeotropically* aligned GH-LCDs (positive contrast) comprising the strongly negative dielectric host N (graph N) and the dual-frequency addressable host M_B (graphs γ and δ) respectively. Graphs α and β are recordings of the transmission characteristics of a *homogeneously* aligned GH-LCD (negative contrast) comprising mixture M_B. The data of mixture N (at 22°C) are: $\eta = 38$ cP, $k_{11} = 14.7 \times 10^{-12}$ N, $k_{22} = 6.93 \times 10^{-12}$ N, $k_{33}/k_{11} = 0.76$, $\varepsilon_{\parallel} = 4.00$, $\Delta\varepsilon = -4.92$, $n_o = 1.482$, $\Delta n = 0.083$, $T_m < -5$°C and $T_{NI} = 63$°C.

Figure 4 was recorded while superimposing the *high-frequency* voltage $V_H = 1.5\ V_{OL} = 4.06$ = volts = constant on V_L; whereas the *low-frequency* voltage $V_L = 2\ V_{OH} = 3.84$ volts = constant was superimposed on V_H upon recording the dashed graph δ. V_{OL} and V_{OH} are the threshold voltages of the respective mechanical deformations of $\hat{n}(M_B)$ in the homogeneous and homeotropic configuration respectively, i.e.

$$V_{OL}(V_H = 0) = \pi(k_{11}/\varepsilon_o\Delta\varepsilon_L)^{1/2} \quad \text{and}$$
$$V_{OH}(V_L = 0) = \pi(k_{33}/\varepsilon_o\Delta\varepsilon_L)^{1/2} \qquad (3)$$

The results in Figure 4 show that negative and positive contrast GH-LCDs comprising M_B can be dual-frequency addressed which leads in both cases to considerably steeper slopes (see graphs β and α as well as δ and γ in Figure 4). It is interesting to note that doping the host mixture M with the black dyes slightly decreases the dielectric cross-over frequency f_c (see data of M and M_B in Table III). As we have shown recently, the shift of the transmission characteristics of dual-frequency addressed GH-LCDs towards higher voltages depends on the dielectric ratio $|\Delta\varepsilon_H|/\Delta\varepsilon_L$ of the host, as well as on V_H/V_{OL} and V_L/V_{OH} respectively.[13]

4. CONCLUSIONS

We have presented four new classes of liquid crystals, each exhibiting distinct physical and electro-optical properties, such as very low viscosities, large mesomorphic temperature ranges, large negative dielectric anisotropies and/or low dielectric relaxation frequencies. Two classes of ethanes were shown to be applicable, for example, in mixtures for high contrast automotive TN-LCDs exhibiting fast total response times $t < 700$ ms at $-20°C$. When temperature compensated with optically active additives, remarkably large multiplexing ratios of $\sim 10:1$ result over extreme operating temperature ranges exceeding 100°C. Due to their low elastic ratios $k_{33}/k_{11} \simeq 1$, conventional time-multiplexing ratios of 32:1 or 64:1 are feasible over temperature ranges 0°C.....50°C with TN-LCDs containing ethanes. Pyridazines exhibit low viscosities despite their large negative dielectric anisotropy $\Delta\varepsilon$. Thus, hosts for positive contrast GH-LCDs comprising them lead to low viscosities $\eta(22°C) = 38$ cP at $\Delta\varepsilon(22°C) = -5$. The fourth class of new compounds, namely the tetracyclic esters, contribute to rather unique static and dynamic dielectric phenomena in dual-frequency addressable mixtures. Thus, mixtures with exceptionally low cross-over frequencies $f_c(22°C) \sim 1$ kHz and large static as well as high-frequency dielectric anisotropies $\Delta\varepsilon_L > +4$ and $\Delta\varepsilon_H < -4$ were achieved that were used in TN-LCDs as well as in positive and negative contrast GH-LCDs. Moreover, we have shown that dual-frequency addressable mixtures comprising such compounds lead to matrix TN-LCDs with remarkably high numbers of multiplexable lines $N_{max} \gg 100$, thus opening up the possibility to realize very high information density TN-LCDs, for example, for computer applications.

Because of the high-frequency capacitive load, dual-frequency addressed LCDs consume higher currents than the presently manufactured low- to medium-information density TN-LCDs. However, the presented new dual-frequency materials lead typically to a specific LCD capacity of ~ 500 pF/cm^2 ($\varepsilon \simeq 5$, $d = 10$ μm). Since, as we have shown, rather low high-frequency driving voltages $V_H(f_H) < 7$ volts[12] are required to increase the number of multiplexable lines of a $2f$-addressed TN-LCD by a factor ~ 30, a specific power consumption of ~ 1.5 mW/cm^2 results for $f_H = 10$ kHz. Thus, considering that the effectively activated electrode area of a dot matrix display is <20% of its total area, the total power consumption of an A4-page sized TN-LCD (21 × 30 cm) becomes $P < 200$ mW. This figure is much smaller than that of any active display and shows that, even with respect to power consumption, the well known

advantages of the passive LCDs can be transferred into the high-information density display field which is at present exclusively dominated by active displays such as CRTs and plasma displays.

References

1. M. Schadt and W. Helfrich, *Appl. Phys. Lett.*, **18**, 127 (1971).
2. G. H. Heilmeier and L. A. Zanoni, *Appl. Phys. Lett.*, **13**, 91 (1968).
3. D. L. White and G. N. Taylor, *J. Appl. Phys.*, **45**, 4718 (1974).
4. T. Uchida, H. Seki, C. Shishido, and M. Wada, *Mol. Cryst. Liq. Cryst.*, **54**, 161 (1979).
5. M. Schadt and P. R. Gerber, *Z. Naturforsch.*, **37a**, 165 (1982) and *Proc. SID*, **23/1**, 29 (1982).
6. A. Boller, H. Scherrer, M. Schadt, and P. Wild, *Proc. IEEE*, **60**, 1002 (1972).
7. G. W. Gray, K. J. Harrison, and J. A. Nash, *Electron. Lett.*, **9**, 98 (1974).
8. R. Eidenschink, D. Erdmann, J. Krause, and L. Pohl, *Angew. Chem.*, **89**, 103 (1977).
9. R. Eidenschink, J. Krause, and L. Pohl, German Patent DE 2636684 (1978).
10. R. Eidenschink, D. Erdmann, J. Krause, and L. Pohl, Proc. 10th Freiburger Arbeitstagung Flüssigkristalle, 26–28 March (1980).
11. K. Praefke, D. Schmidt, and G. Heppke, *Chem. Ztg.*, **104**, 269 (1980).
12. M. Schadt, *Mol. Cryst. Liq. Cryst.*, **83**, 77 (1982).
13. M. Schadt, *Appl. Phys. Lett.*, **41**, 637 (1982).
14. D. Demus, H. J. Deutscher, F. Kuschel, and H. Schubert, DE 2429093 (1973).
15. P. R. Gerber and M. Schadt, *Z. Naturforsch.*, **37a**, 179 (1982).
16. A. Villiger, A. Boller, and M. Schadt, *Z. Naturforsch.*, **34B**, 1535 (1979).
17. G. Meier and A. Saupe, *Mol. Cryst. Liq. Cryst.*, **1**, 515 (1966).
18. A. C. Diogo and A. F. Martins, *Portgal. Phys.*, **11**, 47 (1980).
19. P. Gerber, *Phys. Lett.*, **78A**, 285 (1980).
20. M. Schadt and P. R. Gerber, *Mol. Cryst. Liq. Cryst.*, **65**, 241 (1981).